Inorg. Chem. **2005**, *44*, 3789–3798

Electrochemistry of $[(TMpyP)M^{II}]^{4+}(X^{-})_4$ ($X^- = Cl^-$ or BPh_4^-) and $[(TMpyP)M^{III}Cl]^{4+}(Cl^-)_4$ in *N,N*-Dimethylformamide Where M Is One of 15 Different Metal Ions

E. Van Caemelbecke,[†,‡] A. Derbin,[†] P. Hambright,*[,§] Rachel Garcia,[†] Anass Doukkali,[||] Ahmed Saoiabi,[||] K. Ohkubo,[⊥] S. Fukuzumi,[⊥] and K. M. Kadish*[,†]

Department of Chemistry, University of Houston, Houston, Texas 77204-5641, Houston Baptist University, 7502 Fondren Road, Houston, Texas 77074-3298, Department of Chemistry, Howard University, Washington, D.C. 20059, Laboratoire de Chimie Physique Générale, Département de Chimie, Faculté des Sciences, Université Mohammed V—Agdal, Rabat, Morocco, and Department of Material and Life Sciences, Graduate School of Engineering, Osaka University, Japan

Received August 25, 2004

The electrochemistry of 16 different water-soluble porphyrins of the type $[(TMpyP)M^{II}]^{4+}(X^{-})_4$ or $[(TMpyP)M^{III}Cl]^{4+}(Cl^{-})_4$ is reported in nonaqueous media where TMpyP is the dianion of *meso*-tetrakis(*N*-methylpyridiniumyl)porphyrin and $X^- = Cl^-$ or BPh_4^-. These studies were carried out to examine the effect of the metal ion and porphyrin counterion (X^-) on the electrochemical properties of the TMpyP complexes with a special emphasis being given to the overall number of electrons added and the number of electrode processes upon reduction. All of the investigated compounds with electroinactive central metal ions undergo an overall addition of six electrons. This occurs for most compounds via three two-electron-transfer steps, but more than three processes are observed for porphyrins having metal ions with a low electronegativity (e.g., Cd(II)). The first reduction of each porphyrin having an M(II) ion or an electroinactive M(III) ion yields a porphyrin dianion which is characterized by an intense band located close to 800 nm, and this reversible reduction is followed by further reductions of the 1-methyl-4-pyridyl groups at more negative potentials. Four of the compounds with electroactive central metal ions, $[(TMpyP)M^{III}Cl]^{4+}(Cl^{-})_4$ (M = Co, Fe, Mn, or Au), undergo an additional reversible M(III)/M(II) process prior to reactions involving the porphyrin π-ring system and the 1-methyl-4-pyridyl substituents.

Introduction

Numerous "water-soluble" porphyrins have been studied with respect to their physicochemical and redox properties in both aqueous and nonaqueous media.[1] These compounds have also received considerable attention due to their possible applications in medicine. For example, (5,10,15,20-tetrakis-(1-methyl-4-pyridyl) porphyrins (TMpyP) with specific metal ions have been used in nuclear medicine,[2] tested as tumor and liver contrast agents in mice using magnetic resonance imaging techniques,[3] examined as mimics for superoxide dismutase,[4,5] and shown to act against the human immunodeficiency virus[6] as well as mad-cow disease.[7] More recently, the TMpyPs have been examined for the purpose of developing DNA-specific photosensitizers for photodynamic virus inactivation.[8]

More than 35 different metal ions in up to five different oxidation states (+I, +II, +III, +IV, and +V) have to date

* To whom correspondence should be addressed. E-mail: kkadish@uh.edu (K.M.K.).
‡ Houston Baptist University.
§ Howard University.
|| Université Mohammed V-Agdal.
⊥ Osaka University.
† University of Houston.

(1) Hambright, P. Chemistry of Water Soluble Porphyrins. In *The Porphyrin Handbook*; Kadish, K. M., Smith, K. M., Guilard, R., Eds.; Academic Press: San Diego, CA, 2000; Chapter 18, pp 129–200.
(2) Vaum, R.; Heindel, N. D.; Burns, H. D.; Emrich, J. *J. Pharm. Sci.* **1982**, *71*, 1223.
(3) Ferrer-Sueta, G.; Batinic-Haberle, I.; Spasojevic, I.; Fridovich, I.; Radi, R. *Chem. Res. Toxicol.* **1999**, *12*, 442.
(4) Pasternack, R. F.; Halliwell, B. *J. Am. Chem. Soc.* **1979**, *101*, 1026.
(5) Ilan, Y.; Rabini, J.; Fridovich, I.; Pasternack, R. F. *Inorg. Nucl. Chem. Lett.* **1981**, *17*, 93.
(6) Dixon, D. W.; Schinazi, R.; Marzilli, L. G. *Ann. N.Y. Acad. Sci.* **1990**, *616*, 511.
(7) Caughey, W. S.; Raymond, L. D.; Horiuchi, M.; Caughey, B. *Proc. Natl. Acad. Sci. U.S.A.* **1998**, *95*, 12117.

10.1021/ic048820q CCC: $30.25
Published on Web 05/13/2005

Chart 1

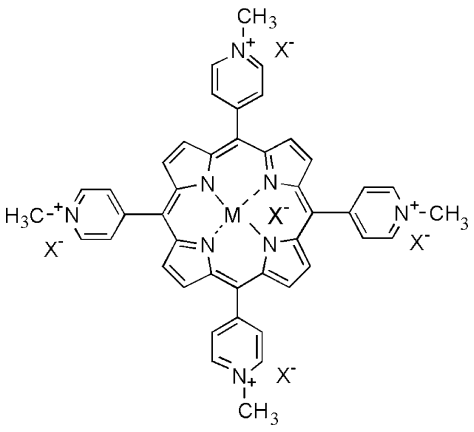

been incorporated[1] into the central cavity of H_2TMpyP which exists as a tetracation in its free base form. The metalated compounds in their neutral form are represented as $[(P)M^{II}]^{4+}(X^-)_4$, $[(P)M^{III}X]^{4+}(X^-)_4$, or $[(P)M^{IV}X_2]^{4+}(X^-)_4$ where the X^- anion ($X^- = Cl^-$, ClO_4^-, or $CH_3C_6H_4SO_3^-$) is associated with the four positively charged 1-methyl-4-pyridyl groups and possibly also coordinated to the central metal ion depending on its oxidation state (see Chart 1 for M(III) complex).

Many electron transfer reactions of the TMpyP derivatives have been examined in aqueous media utilizing classical electrochemistry or pulse radiolysis[1,9−17] while others have been electrochemically investigated in nonaqueous media, most often with cyclic voltammmetry.[18−21] In nonaqueous media, multiple electron transfer reactions can be detected due to the increased solvent range of the nonaqueous solvent as compared to water. These later studies have shown that porphyrins with TMpyP macrocycles can be reduced not only at the metal center but also at the conjugated π-ring system and at the four 1-methyl-4-pyridyl substituents.

Electrochemical studies in aqueous solutions have led to the conclusion that TMpyP derivatives which contain an M(II) or an electroinactive M(III) ion are initially reduced at the π-ring system to give a π-anion radical.[9,10,12,14] The electrogenerated π-anion radical is usually unstable in water and ultimately converted to a phlorin or chlorin.[10,14] A proposed mechanism for this chemical reaction involves disproportionation of the π-anion radical followed by abstraction of protons from the solvent by the dianionic species. Despite what is seen in aqueous media, electrochemical studies of the same compounds in nonaqueous media[18−21] (such as DMF, DMSO, or py) have suggested several different types of electron transfer mechanisms. For example, one investigated compound, $[(TMpyP)Ni]^{4+}(ClO_4^-)_4$, was proposed to exist in both a monomeric and dimeric form in DMF containing 0.1 M TBAP and under these conditions was reduced by four one-electron-transfer steps.[18] In contrast, $[(TMpyP)Zn]^{4+}(SO_3C_6H_4CH_3^-)_4$ and $[(TMpyP)Cu]^{4+}$-$(SO_3C_6H_4CH_3^-)_4$, both of which have electroinactive M(II) central metal ions, exist only in their monomeric form in DMF, 0.1 M TBAP, and these porphyrins are reduced in three well-defined two-electron-transfer steps.[19]

The Zn(II) and Cu(II) derivatives of TMpyP both have electroinactive metal ions while Ni(II) can, under the same conditions, be reduced to Ni(I).[22] This might be one reason for the different reported behavior of the three types of TMpyP complexes. A second reason for the difference might be the different counterions of the investigated compounds, i.e., ClO_4^- in one case and $SO_3C_6H_4CH_3^-$ in another, or it could be simply related to a difference in the electroactive character of the metal ions.

The type and size of counterion should be irrelevant in water since porphyrins with a TMpyP ring containing an M(II) or M(III) metal ion should exist in their dissociated form, i.e., $[(TMpyP)M^{II}]^{4+}$ instead of $[(TMpyP)M]^{4+}(X^-)_4$ and $[(TMpyP)M^{III}X]^{4+}$ instead of $[(TMpyP)M^{III}X]^{4+}(X^-)_4$ under these solution conditions. In contrast, the type of counterion on the porphyrin moiety might affect the electrochemistry in nonaqueous solvents such as DMF, DMSO, or pyridine where the associated form may predominate in solution over the dissociated form due to the low polarity of the solvent.

One main point of this paper is to elucidate the electrochemistry of TMpyP complexes with many different metal ions as was previously done for derivatives of TPP, OEP, Br_8TPP, and other macrocycles.[22] However, the effect of counterion is also investigated in the present study which reports the electrochemistry of 16 different complexes of the type $[(TMpyP)M]^{4+}(X^-)_4$ and $[(TMpyP)MCl]^{4+}(Cl^-)_4$ where M is an M(II) or M(III) metal ion (see the periodic table for metal ions investigated) and $X^- = Cl^-$ or BPh_4^-. More specifically, we have examined how the type of metal ion and/or counterion on the TMpyP macrocycle can influence both the overall number of electrons added to the porphyrin moiety and the number of electron transfer steps. The current work is carried out in DMF and extends the electrochemistry of metalloporphyrins with a TMpyP macrocycle in nonaqueous media to complexes with either fourth, fifth, or sixth row transition metal ions.

(8) Zupan, K.; Herenyi, L.; Toth, K.; Majer, Z.; Csik, G. *Biochemistry* **2004**, *43*, 9151.
(9) Baral, S.; Hambright, P.; Neta, P. *J. Phys. Chem.* **1984**, *88*, 1595.
(10) Richoux, M.-C.; Neta, P.; Harriman, A.; Baral S.; Hambright, P. *J. Phys. Chem.* **1986**, *90*, 2462.
(11) Harriman, A.; Richoux, M.-C.; Neta, P. *J. Phys. Chem.* **1983**, *87*, 4957.
(12) Kalyanasundaram, K.; Neumann-Spallart, M. *J. Phys. Chem.* **1982**, *86*, 5163.
(13) Abou-Gamra, Z. M.; Harriman, A.; Neta, P. *J. Chem. Soc., Faraday Trans. 2* **1986**, 2337.
(14) Abou-Gamra, Z. M.; Guindy, N. *Spectrochim. Acta* **1989**, *45A*, 1207.
(15) Bettelheim, A.; Kuwana, T. *Anal. Chem.* **1979**, *51*, 2257.
(16) Morehouse, K. M.; Neta, P. *J. Phys. Chem.* **1984**, *88*, 1575.
(17) Hambright, P.; Neta, P.; Richoux, M.-C.; Abou-Gamra, Z. M.; Harriman, A. *J. Photochem.* **1987**, *36*, 255.
(18) Kadish, K. M.; Sazou, D.; Liu, M.; Saoiabi, A.; Ferhat, M.; Guilard, R. *Inorg. Chem.* **1988**, *27*, 686.
(19) Kadish, K. M.; Araullo, C.; Maiya, G. B.; Sazou, D.; Barbe, J. M.; Guilard, R. *Inorg. Chem.* **1989**, *28*, 2528.
(20) Araullo-Mc Adams, C.; Kadish, K. M. *Inorg. Chem.* **1990**, *29*, 2749.
(21) Van Caemelbecke, E.; Kutner, W.; Kadish, K. M. *Inorg. Chem.* **1993**, *32*, 438.
(22) Kadish, K. M.; Van Caemelbecke, E.; Royal, G. Electrochemistry of Metalloporphyrins in Nonaqueous Media. In *The Porphyrin Handbook*; Kadish, K. M., Smith, K. M., Guilard, R., Eds.; Academic Press: San Diego, CA, 2000; Chapter 55, pp 1−114.

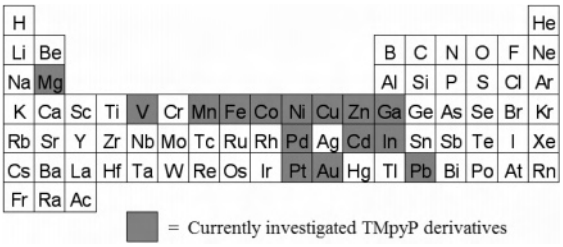

Experimental Section

Chemicals. High purity N_2 gas was purchased from Matheson-Trigas. Anhydrous argon-packed *N*,*N*-dimethylformamide was obtained from Aldrich Chemical Co. and was used without further purification. Tetra-*n*-butylammonium perchlorate (TBAP) was purchased from Fluka Chemika Co., recrystallized from ethyl alcohol, and dried under vacuum at 40 °C for at least one week prior to use. All investigated metalloporphyrins with the exception of $[(TMpyP)Pb]^{4+}(BPh_4^-)_4$, $[(TMpyP)Cd]^{4+}(BPh_4^-)_4$, and $[(TMpyP)Zn]^{4+}(BPh_4^-)_4$ were purchased from Mid-century Chemicals (Posen, IL) and were used as received. Synthesis and characterization of the Pb, Cd, and Zn derivatives is described below.

Synthesis of (TMpyP)Zn(SO$_3$C$_6$H$_4$CH$_3$)$_4$. $(TMpyP)H_2(SO_3C_6H_4CH_3)_4$ (0.2 g, 1.46×10^{-4} mol) and 0.2 g of $ZnCl_2$ (1.49×10^{-3} mol) were added to 100 mL of DMF, and the solution slowly warmed while being stirred. The reaction was complete after 1 h after which the solution was concentrated by slow evaporation. The product was then purified on an alumina column using ethanol as eluent. The fraction collected was completely dried, and the solid residue was washed with hexane.

Synthesis of (TMpyP)Cd(BPh$_4$)$_4$. A mixture of 0.2 g of $(TMpyP)H_2(SO_3C_6H_4CH_3)_4$ (1.46×10^{-4} mol) and 0.34 g of $CdCl_2$ (1.5×10^{-3} mol, solubilized in 150 mL of DMF) was warmed to 100 °C using a water bath. The reaction was completed in 30 min. Ethanol (150 mL) was added to the solution and stirred gently at room temperature for an hour. The precipitate which formed was collected and washed with acetone.

Synthesis of (TMpyP)Pb(BPh$_4$)$_4$. $(TMpyP)H_2(SO_3C_6H_4CH_3)_4$ (0.2 g, 1.46×10^{-4} mol) and 0.48 g of $Pb(CH_3COOH)_2 \cdot 3H_2O$ were dissolved in 150 mL of DMF. The solution was stirred as it was warmed to increase the rate of reaction. Ethanol was added to the solution while stirring, and the precipitate that formed under these conditions was collected and washed with hexane.

Unlike (TMpyP)Zn, the (TMpyP)M derivatives with M = Cd or Pb could not be further purified on a silica column owing to their decomposition on the column. Another method of purification was therefore designed in which the porphyrins were made water-insoluble in order to solubilize excess salt and consequently eliminate it, as was previously done for a series of (TpyP)M compounds.[23] In this paper, the counterion on the $[(TMpyP)]^{4+}$ moiety, $(p\text{-}SO_3C_6H_4CH_3)^-$, was replaced by a more lipophilic counterion, BPh_4^-. To an aqueous solution of $(TMpyP)M(SO_3C_6H_4CH_3)_4$ (M = Pb or Cd) was added an equimolar amount of $NaBPh_4$ (soluble in water) while stirring. The reaction was fast, and the $(TMpyP)M(BPh)_4$ product appeared as a suspension in water. The solution was placed in a separatory funnel to which was added excess water and CH_2Cl_2. The metalloporphyrin was collected in the organic phase as an emulsion and washed with hot water and heptane. The solid residue was then dried in a vacuum oven.

Although not necessary for the purification of (TMpyP)Zn-$(SO_3C_6H_4CH_3)$, the porphyrin counterion, $(p\text{-}SO_3C_6H_4CH_3)^-$, was substituted by BPh_4^- in a way similar to the one described above for the purification of the Cd(II) and Pb(II) derivatives in order to obtain a series of TMpyP complexes having the same counterion.

Spectral Characterization of (TMpyP)M(BPh$_4$) (M = Zn, Cd, or Pb). UV−vis data in DMF: λ/nm ($\epsilon \times 10^{-3}$/mol^{-1} L cm^{-1}), M = Zn, 446 (113.4), 566 (10), 612 (1.7); M = Cd, 460 (90.4), 589 (3.1), 637 (2); M = Pb, 362 (22), 478 (79.8), 611 (2), 663 (3.5).

^{1}H NMR spectral data ($CDCl_3$): M = Zn, 4.75 (s, 12H, N−CH_3), 8.93 and 8.96 (d, 8H, α-H), 9.44 and 9.47 (d, 8H, *β*-H), 9.11 (s, 8H, H_{pyrr}), 7.22 (m, 32H, BPh_4), 6.97 (t, 32H, BPh_4), and 6.83 (t, 16H, BPh_4); M = Cd, 4.74 (s, 12H, N−CH_3), 8.90 (d, 8H, α-H), 9.43 (d, 8H, *β*-H), 8.97 (s, 8H, H_{pyrr}), 7.21 (m, 32H, BPh_4), 6.97 (t, 32H, BPh_4), and 6.83 (t, 16H, BPh_4); M = Pb, 4.75 (s, 12H, N−CH_3), 8.90 and 8.94 (d, 8H, α-H), 9.43 and 9.47 (d, 8H, *β*-H), 9.16 (s, 8H, H_{pyrr}), 7.21 (m, 32H, BPh_4), 6.96 (t, 32H, BPh_4), 6.82 (t, 16H, BPh_4).

Mass spectral data [*m*/*e* (fragment)]: M = Zn, 742 [(TMpyP)-Zn]$^+$, 727 [(TMpyP)Zn − (CH_3)]$^+$, 712 [(TMpyP)Zn − 2(CH_3)]$^+$, 697 [(TMpyP)Zn − 3(CH_3)]$^+$; M = Cd, 790 [(TMpyP)Cd + 2H]$^+$, 788 [(TMpyP)Cd]$^+$, 774 [(TMpyP)Cd − (CH_3) + H]$^+$, 758 [(TMpyP)Cd − 2(CH_3)]$^+$, 743 [(TMpyP)Cd − 3(CH_3)]$^+$, 680 [(TMpyP) + 4H]$^+$, 666 [(TMpyP) − (CH_3) + 5H]$^+$; M = Pb, 884 [(TMpyP)Pb]$^+$, 868 [(TMpyP)Pb − (CH_3) − H]$^+$, 853 [(TMpyP)Pb − 2(CH_3) − H]$^+$, 839 [(TMpyP)Pb − 3(CH_3)]$^+$, 680 [(TMpyP) + 4H]$^+$.

IR spectral data (cm^{-1}): M = Zn, 3051 [*ν*(CH aromatic)], 1632 [*ν*(C=N pyrr)], 1578, 1530 and 1478 [*ν*(C−C aromatic)], 1426 [*δ*(CH_3)], 790 [*δ*(CH pyrr)], 734 and 705 [*δ*(CH *meso*-phenyl)]; M = Cd, 3051 [*ν*(CH aromatic)], 1631 [*ν*(C=N pyrr)], 1578, 1517 and 1478 [*ν*(C−C aromatic)], 1426 [*δ*(CH_3)], 787 [*δ*(CH pyrr)], 734 and 706 [*δ*(CH *meso*-phenyl)]; M = Pb, 3051 [*ν*(CH aromatic)], 1633 [*ν*(C=N pyrr)], 1578, 1521 and 1478 [*ν*(C−C aromatic)], 1425 [*δ*(CH_3)], 790 [*δ*(CH pyrr)], 733 and 705 [*δ*(CH *meso*-phenyl)].

Instrumentation. Cyclic, normal pulse, and differential pulse voltammetry were carried out using either an EG&G Princeton Applied Research (PAR) model 173 potentiostat coupled to an EG&G model 175 universal programmer, an EG&G model 263 potentiostat/galvanostat, or an EC 225[2A] voltammetric analyzer from IBM Instruments Inc. A conventional three-electrode cell was used and consisted of a glassy carbon electrode as working electrode, a platinum wire as counter electrode, and a homemade saturated calomel reference electrode (SCE). The SCE was separated from the solution by a fritted glass bridge of low porosity that contained the solvent and the supporting electrolyte.

Nitrogen gas was used to deoxygenate the solutions for 5 min or more prior to each electrochemical experiment, and a blanket of the gas was maintained over the solution throughout the measurement. The supporting electrolyte was 0.1 or 0.2 M TBAP for cyclic voltammetry and 0.1 or 0.2 M TBAP for spectroelectrochemical measurements. Ferrocene was used as the internal standard in all electrochemical experiments. The Fc/Fc^+ redox couple was located at $E_{1/2}$ = +0.54 V versus SCE in DMF containing 0.1 M TBAP.

UV−vis spectroelectrochemical experiments were performed with a home-built thin-layer cell[24] that had a light-transparent platinum gauze as a working electrode. Potentials were applied and monitored with an EG&G model 173 potentiostat. Time-dependent

(23) Doukkali, A. Ph.D. Thesis, Université Mohammed V−Agdal, Faculté des Sciences de Rabat, Morocco, 2002.

(24) Lin, X. Q.; Kadish, K. M. *Anal. Chem.* **1985**, *57*, 1498.

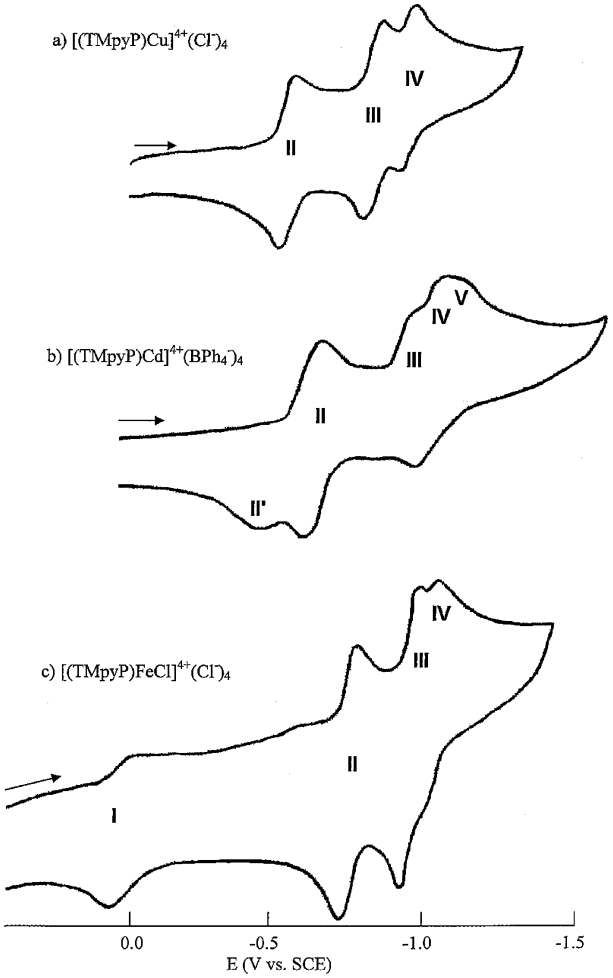

Figure 1. Cyclic voltammograms of (a) $[(TMpyP)Cu]^{4+}(Cl^-)_4$, (b) $[(TMpyP)Cd]^{4+}(BPh_4^-)_4$, and (c) $[(TMpyP)FeCl]^{4+}(Cl^-)_4$ in DMF, 0.1 M TBAP. Scan rate = 0.1 V/s.

UV−vis spectra were recorded on a Hewlett-Packard model 8453 diode array spectrophotometer.

The ESR spectrum of the reduced gold porphyrin was measured in frozen DMF under nonsaturating microwave power conditions with a JEOL X-band spectrometer (JES-RE1XE) using an attached variable temperature apparatus. The *g* values were calibrated with a Mn^{2+} marker. ^1H NMR spectra were measured at a frequency of 200 MHz on a Bruker AC 200. Spectra were typically recorded with 5 mg sample in 0.5 cm^3 $CDCl_3$ using TMS as internal reference. Mass spectra were obtained by MALDI (matrix assisted laser desorption ionization) in positive mode with samples dissolved in DMF. IR spectra were recorded as KBr pellets between 400 and 4000 cm^{-1} on a Bruker IFS 66v.

Results and Discussion

The 16 different metalloporphyrins investigated in this study can be divided into three groups on the basis of their electrochemical behavior in DMF containing 0.1 M TBAP. The first group of compounds undergoes three well-defined two-electron transfers with no associated chemical reactions as illustrated in Figure 1a for $[(TMpyP)Cu]^{4+}(Cl^-)_4$ in DMF, 0.1 M TBAP. A similar result was reported for $(TMpyP)M(SO_3C_6H_4CH_3)_4$ (M = Zn, Cu, or VO) under the same solution conditions.[19] The second group of compounds is characterized by the presence of coupled chemical reactions, and the voltammograms resemble those illustrated in Figure 1b for the case of $[(TMpyP)Cd]^{4+}(BPh_4^-)_4$. The third group of compounds contains those which exhibit a reversible one-electron metal-centered reduction in an initial step and multielectron transfers at more negative potentials as previously illustrated in the case of $[(TMpyP)MnCl]^{4+}(Cl^-)_4$.[21] This electrochemical behavior is shown in Figure 1c for the case of $[(TMpyP)FeCl]^{4+}(Cl^-)_4$. For the purpose of discussion, the three groups in the present paper are called groups A, B, and C. Table 1 lists half-wave potentials for each redox reaction as well as gives the absolute potential separation between the first two multielectron reductions labeled as Δ_1 and between the next two multielectron reductions labeled as Δ_2.

Electrochemistry. As shown in Table 1, the porphyrins in group A have values of Δ_1 (III−II) which range from 0.25 V ($M = Pt^{II}$) to 0.38 V ($M = In^{III}$) and values of Δ_2 (IV−III) which range from 0.06 V ($M = Ga^{III}$) to 0.19 V ($M = In^{III}$), thus giving a Δ_1 (III−II) which is larger than Δ_2 (IV−III) by 0.06−0.32 V. In addition, the absolute value of $\Delta_1 - \Delta_2$ varied from 0.15 to 0.25 V.

Three reversible reductions, each involving a transfer of two electrons, have been reported for $[(TMpyP)M](CH_3C_6H_4SO_3)_4$ (M = VO, Zn, and Cu) in DMF containing 0.1 M TBAP as supporting electrolyte.[19] All compounds in group A exhibit an electrochemical behavior in DMF similar to what has been reported for the above compounds under the same solution conditions[19] (see Table 1 and Figure 1a), thus suggesting that two electrons are transferred during each reduction of the compound.

Confirmation of this result for the case of $[(TMpyP)VO]^{4+}(Cl^-)_4$ is illustrated in Figure 2 which shows the cyclic voltammogram, differential pulse voltammogram, and normal pulse voltammogram of the compound in DMF 0.1 M TBAP. The theoretical value of $|E_{pc} - E_{pa}|$ by cyclic voltammetry is $59/n$ mV for a reversible electron transfer, and one would therefore expect a difference in peak potentials of ca. 30 mV for processes II, III, and IV if each electrode reaction involved a transfer of two electrons. The value of $|E_{pc} - E_{pa}|$ for process II in Figure 2a is 33 mV, which indicates that $[(TMpyP)VO]^{4+}(Cl^-)_4$ is initially reduced by two electrons. The normal pulse voltammogram exhibits three steps of similar height. Wave analyses of processes II, III, and IV give respectively 35, 32, and 31 mV for $|E_{3/4} - E_{1/4}|/n$ mV which corresponds to a transfer of two electrons during each reduction. Furthermore, the differential pulse voltammogram of the compound in Figure 2b shows three processes of similar peak width that agrees with the same number of electrons transferred during II, III, and IV. Overall, the data in Figure 2 are self-consistent, and a total of six electrons are transferred for the reduction−oxidation processes of $[(TMpyP)VO]^{4+}(Cl^-)_4$.

The porphyrins in group B exhibit two or three reduction peaks following process II (labeled as III, IV, and V in Table 1) as opposed to only two for the seven compounds in group A. Figure 3 illustrates cyclic voltammograms of the Mg, Cd, and Zn derivatives in DMF, 0.1 M TBAP. In each case, an additional process (labeled as II′ in Figure 3) is observed on

Table 1. Half-Wave Potentials ($E_{1/2}$ in V vs SCE) of Investigated TMpyP Complexes in DMF, 0.1 M TBAP

	metal ion[a]		reductions			1-methyl-4-pyridyl				Δ_1(V)	Δ_2(V)
group	M	EN[b]	M^{III}/M^{II} I (ne^-)	M^{II}/M^{I} I′(ne^-)	π-ring II (ne^-)	III	IV	V	(ne^-)[g]	(III−II)	(IV−III)
A	In^{III}	1.45			−0.44 (2)	−0.82	−1.01		(4)	0.38	0.19
	$V^{IV}O$	1.74			−0.48 (2)	−0.83	−0.97		(4)	0.35	0.14
	Pt^{II}	1.54			−0.67 (2)	−0.92	−1.02		(4)	0.25	0.10
	Pd^{II}	1.52			−0.56 (2)	−0.83	−0.95		(4)	0.27	0.12
	Cu^{II}	1.62			−0.60 (2)	−0.87	−0.97		(4)	0.27	0.10
	Ni^{II}	1.57			−0.45 (2)	−0.78	−0.91		(4)	0.33	0.13
	Ga^{III}	1.52			−0.46 (2)	−0.77	−0.83		(4)	0.31	0.06
B	Zn^{II}	1.48			−0.65 (2)	−1.02	−1.10[d]		(4)	0.37	0.08
	Mg^{II}	1.24			−0.63 (2)	−1.02	−1.08[d]	−1.31[d]	(4)	0.39	0.06
	Pb^{II} [c]	1.17			−0.53 (2)	−0.92[d]				0.39	
	Cd^{II} [c]	1.34			−0.65 (2)	−0.94[d]	−1.05[d]	−1.12[d]	(4)	0.29	0.11
C	Mn^{II}	1.45	0.08 (1)		−0.71 (2)	−0.91	−1.07	−1.18	(4)	0.20	0.16
	Fe^{II}	1.50	0.00 (1)		−0.74 (2)	−0.93	−1.01		(4)	0.19	0.08
	Au^{II}	*e*	−0.20 (1)	−0.36[f](1)		−0.60	−0.70		(4)		0.10
	Co^{II}	1.54	0.49 (1)	−0.49 (1)	−0.71 (2)	−0.89	−0.98		(4)	0.18	0.09

[a] The counteranion is Cl^- unless otherwise indicated. [b] Calculated as described in ref 33. [c] The counterion on the $N-CH_3^+$ group is BPh_4^-. [d] E_{pc} values at 0.1 V/s. [e] Could not be determined. [f] Generation of Au^I species is not confirmed. [g] Number of electrons involved in process III + IV + V.

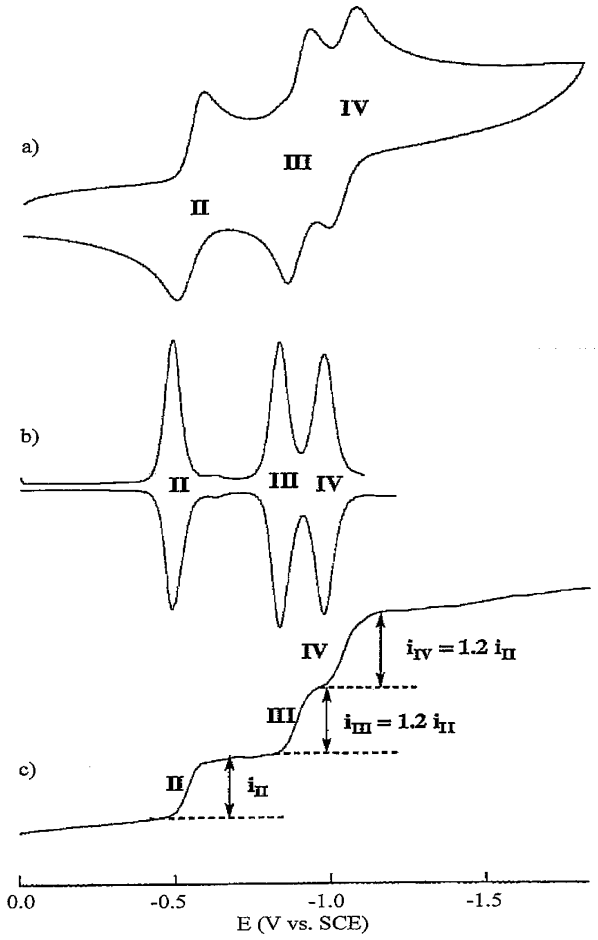

Figure 2. (a) Cyclic, (b) differential pulse, and (c) normal pulse voltammogram of $[(TMpyP)VO]^{4+}(Cl^-)_4$ in DMF, 0. 1 M TBAP.

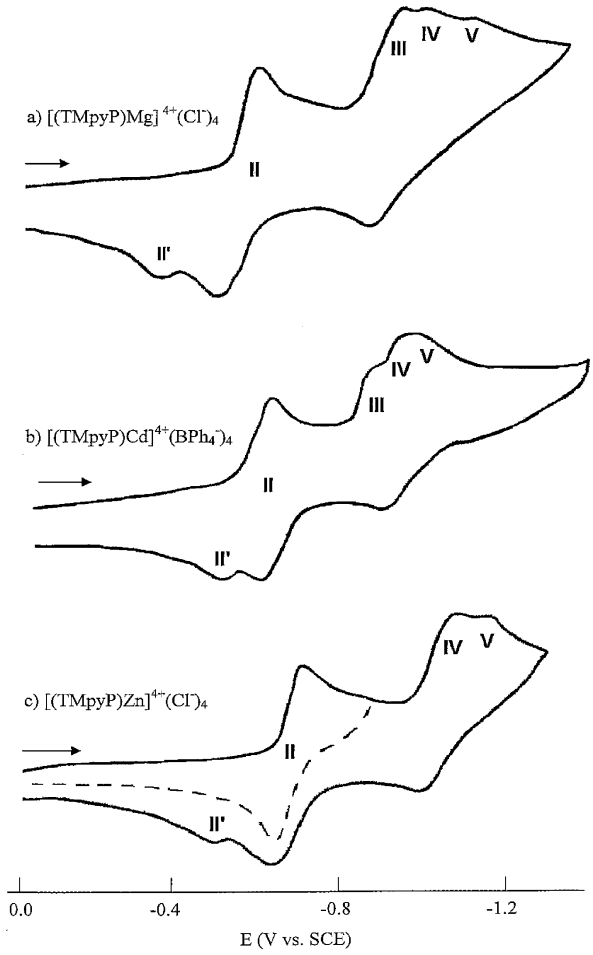

Figure 3. Cyclic voltammograms of (a) $[(TMpyP)Mg]^{4+}(Cl^-)_4$, (b) $[(TMpyP)Cd]^{4+}(BPh_4^-)_4$, and (c) $[(TMpyP)Zn]^{4+}(Cl^-)_4$ in DMF, 0.1 M TBAP. Scan rate = 0.1 V/s. The dashed line in part c was obtained by reversing the potential scan prior to process IV.

the anodic sweep when the potential scan is reversed at a potential more negative than process V. This peak is not seen when the scan is reversed immediately after process II (see dashed line in Figure 3c for the case of the Zn derivative). In addition, the three processes III, IV, and V have different peak current heights, and the ratios of peak currents between these three processes vary with the type of metal ion, i.e., Mg, Cd, or Zn (see Figure 3). The normal pulse voltammograms of $[(TMpyP)Zn]^{4+}(BPh_4^-)_4$, $[(TMpyP)Pb]^{4+}(BPh_4^-)_4$, and $[(TMpyP)Cd]^{4+}(Cl^-)_4$ are illustrated as representative examples in Figure 4. In each case, there are two steps, the second of which has a height approximately double the first step. Wave analysis yields a range of values for $|E_{3/4} - E_{1/4}|$ from 30 to 38 mV for the first step (process II) of each of

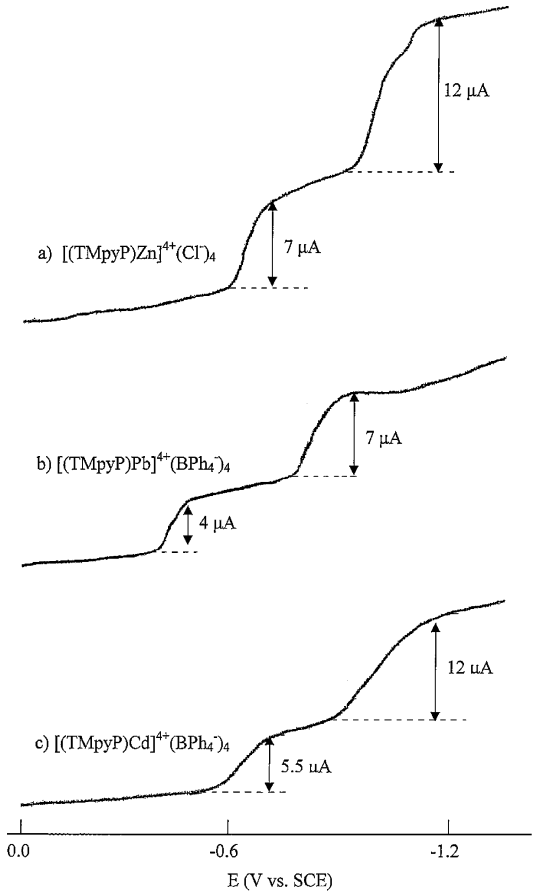

Figure 4. Normal pulse voltammograms of 1×10^{-3} M (a) [(TMpyP)-Zn]$^{4+}$(Cl$^-$)$_4$, (b) [(TMpyP)Pb]$^{4+}$(BPh$_4^-$)$_4$, and (c) [(TMpyP)Cd]$^{4+}$(BPh$_4^-$)$_4$ in DMF, 0.1 M TBAP.

the three compounds, which indicates a two-electron transfer. Since the second step (a combination of processes III and higher) is double in height of the first, it must involve four electrons. The first reductions of the three compounds by cyclic voltammetry are characterized by an $|E_{pc} - E_{pa}|$ of 34−40 mV, thus consistent with an electrode reaction involving a transfer of two electrons in the first step. Therefore, the combined cyclic voltammetry and normal pulse voltammetry data indicate that all three derivatives in Figure 4 are reduced by an overall six electrons.

This number of electrons is also proposed to be transferred upon reduction of [(TMpyP)Mg]$^{4+}$(Cl$^-$)$_4$, on the basis of similarities between the cyclic voltammograms in Figure 3.

Cyclic voltammograms of each group C compound in DMF, 0.1 M TBAP, are illustrated in Figure 5. All four derivatives in group C undergo more than three reductions, the first of which occurs in the range of $E_{1/2}$ between +0.49 V (in the case of cobalt) and −0.20 V (in the case of Au) as seen in Table 1. The reductive behavior of the Mn and Co derivatives has previously been discussed in the literature. In each case, the first electrode process of the compound was assigned to the M(III)/M(II) redox couple.[20,21] On the basis of this result and similarities between the voltammograms, we propose that the other two complexes in Figure 5 (Fe(III) and Au(III)) are also reduced at the metal center prior to electron transfer involving the porphyrin macrocycle and/or the 1-methyl-4-pyridyl groups.

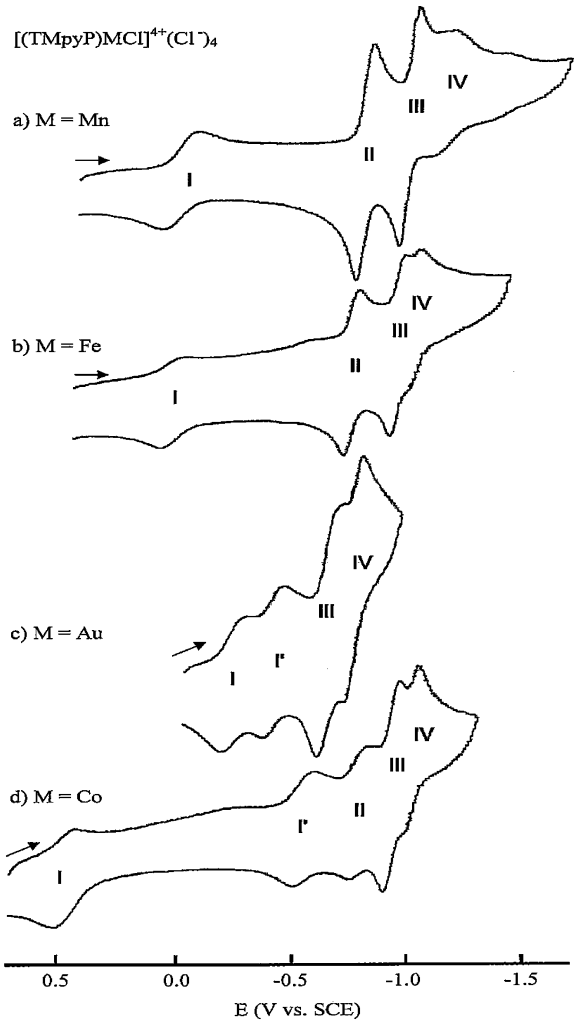

Figure 5. (a) Cyclic voltammogram of [(TMpyP)MCl]$^{4+}$(Cl$^-$)$_4$ (M = Fe, Mn, Co, or Au) in DMF, 0.1 M TBAP. Scan rate = 0.1 V/s.

The three electrode reactions of [(TMpyP)FeCl]$^{4+}$(Cl$^-$)$_4$ which occur at potentials negative of the metal-centered process exhibit current−voltage curves that resemble those of the group A compounds (see Figure 1), thus suggesting that six electrons are added to the porphyrin after the initial Fe(III)/Fe(II) process. Three electrode processes are also observed after the first reduction of [(TMpyP)AuCl]$^{4+}$(Cl$^-$)$_4$, but in this case, the first and the second reductions have a similar peak current height and peak to peak separation close to 60 mV (see Figure 5), thus suggesting that both reductions involve the transfer of one electron. The last two reductions of [(TMpyP)AuCl]$^{4+}$(Cl$^-$)$_4$ have a higher peak current height than the first two reductions of the same compound and a smaller ΔE_p, thus suggesting a transfer of two electrons in each of the last two processes at $E_{1/2} = -0.60$ and −0.70 V.

Metalloporphyrins containing a gold(III) central metal ion were initially thought to undergo two consecutive ring-centered electrode reactions to give ultimately a gold(III) porphyrin dianion,[22] but more recent studies now show that the electrode reactions actually occur at the metal center.[25]

Ag(III) porphyrins also undergo a Ag(III)/Ag(II) process as well as a Ag(II)/Ag(I) reaction[26,27] prior to reduction at

the conjugated macrocycle while copper porphyrins are all stable in the Cu(II) oxidation state.[22] Thus, it is highly likely that a Au(II) complex is the first reduction product of $[(TMpyP)AuCl]^{4+}(Cl^-)_4$ and a Au(I) species may also be possible in light of comparison with data on the Ag complexes. Unfortunately, one cannot distinguish solely on the basis of cyclic voltammetry whether the first reduction of $[(TMpyP)AuCl]^{4+}(Cl^-)_4$ involves the porphyrin macrocycle or the metal center, and this point was further examined by combined UV−vis spectroelectrochemistry and ESR spectroscopy as described in later sections of this paper.

Effect of Counterion. Four selected TMpyP derivatives (three in group A and one in group B) were investigated as to the effect of counterion on the number of redox processes and their $E_{1/2}$ values. The Cu, Ni, and VO derivatives investigated in this study all have Cl^- as counterion, and the data for these derivatives can be compared with that of previously investigated $[(TMpyP)M]^{4+}(CH_3C_6H_4SO_3^-)_4$ (M = Cu or VO)[19] and $[(TMpyP)Ni]^{4+}(ClO_4^-)_4$.[18] The Zn porphyrins investigated in the present study were synthesized with two types of counterions, Cl^- and BPh_4^-, and their electrochemical behavior can be compared to that of $[(TMpyP)Zn]^{4+}(CH_3C_6H_4SO_3^-)_4$ whose electrochemistry has previously been reported in the literature.[19]

The Cu and VO porphyrins show virtually no effect of the counterion on the number of redox processes, and both the presently investigated Cl^- derivatives and the earlier characterized $CH_3C_6H_4SO_3^-$ derivatives[19] undergo three reversible two-electron transfers. The $E_{1/2}$ values for each reaction of the copper complex (−0.60, −0.87, and −0.97 V for $[(TMpyP)Cu]^{4+}(Cl^-)_4$ as compared to −0.61, −0.89, and −1.02 V for $[(TMpyP)Cu]^{4+}(CH_3C_6H_4SO_3^-)_4$) are also virtually independent of the type of counteranion (Cl^- or $CH_3C_6H_4SO_3^-$) assuming an uncertainty in the measurement of ±0.01 V. This is also the case for the VO porphyrin. The Cl^- derivative exhibits three reductions at −0.48, −0.83, and −0.97 V as compared to −0.52, −0.85, and −1.01 V for the $CH_3C_6H_4SO_3^-$ derivative.[19]

However, there is a clear effect of the counterion in the case of the Ni porphyrins. $[(TMpyP)Ni]^{4+}(Cl^-)_4$ exhibits three reversible redox reactions (see Table 1) which parallels what is observed for other group A porphyrins examined in the present study. These results contrast with what has been reported for $[(TMpyP)Ni]^{4+}(ClO_4^-)_4$; in this case, the neutral and reduced forms of this compound were proposed to exist in a monomer−dimer equilibrium in DMF, and this equilibrium resulted in four one-electron reductions at $E_{1/2}$ = −0.51, −0.61, −0.84, and −0.97 V vs SCE.[18]

Figure 6 compares the cyclic voltammograms of $[(TMpyP)Zn]^{4+}(BPh_4^-)_4$ and $[(TMpyP)Zn]^{4+}(Cl^-)_4$ to the cyclic voltammogram of $[(TMpyP)Zn]^{4+}(CH_3C_6H_4SO_3^-)_4$ which has been previously reported in the literature.[19] Four reduction peaks are seen for $[(TMpyP)Zn]^{4+}(BPh_4^-)_4$ as compared to only three for $[(TMpyP)Zn]^{4+}(Cl^-)_4$ and $[(TMpyP)Zn]^{4+}(CH_3C_6H_4SO_3^-)_4$. In addition, the last two processes of the $CH_3C_6H_4SO_3^-$ derivative are reversible, but this is not the case for the other two compounds in Figure 6. Also, process II′ is very apparent in Figure 6a while it is of very small magnitude in Figure 6b and does not exist in Figure 6c. These data thus show that the current−voltage curves for reduction of the zinc complexes depend on the porphyrin counterion.

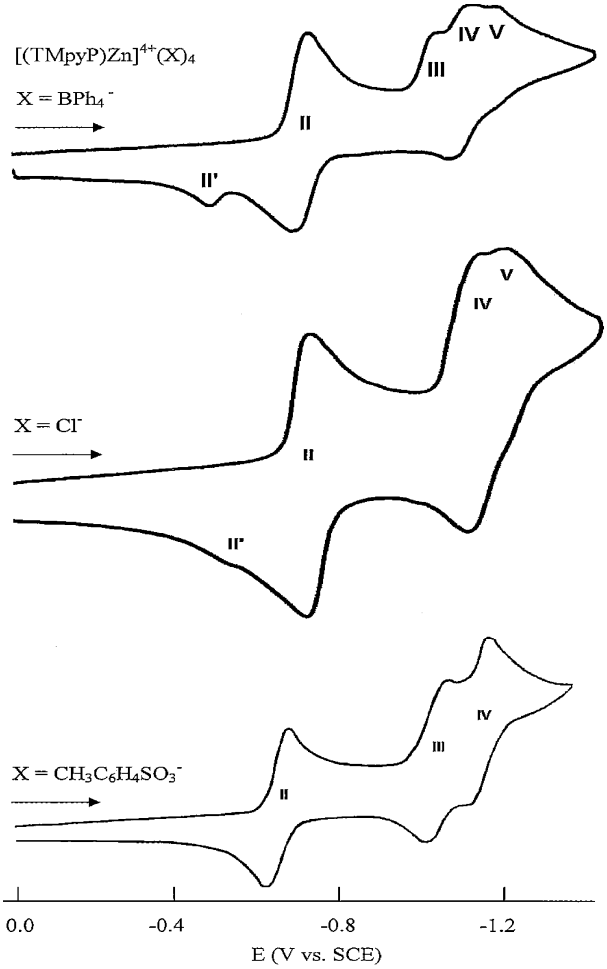

Figure 6. Cyclic voltammograms of (a) $[(TMpyP)Zn]^{4+}(BPh_4^-)_4$, (b) $[(TMpyP)Zn]^{4+}(Cl^-)_4$, and (c) $[(TMpyP)Zn]^{4+}(CH_3C_6H_4SO_3^-)_4$ in DMF, 0.2 M TBAP. Scan rate = 0.1 V/s.

UV−Vis Spectroelectrochemistry. The first two-electron reduction of $[(TMpyP)M]^{4+}(Cl^-)_4$ (M = Cu, Zn, or VO) is reversible by thin-layer cyclic voltammetry, and the UV−vis spectral changes obtained upon the first two-electron reduction of the VO and Zn complexes are illustrated in Figure 7a,b. Similar spectral changes are observed for the other compounds, and the resulting data are summarized in Table 2. As the reduction of $[(TMpyP)M]^{4+}(Cl^-)_4$ (M = VO or Zn) proceeds in the thin-layer cell, the Soret band decreases in intensity, and two new bands of similar height grow in at 469−491 and 772−857 nm (see Figure 7). The net addition of two electrons on the porphyrin ring should yield a porphyrin dianion. Spectral characterizations of these

(25) (a) Kadish, K. M., Wenbo, E.; Ou, Z.; Shao, J.; Sintic, P. J.; Ohkubo, K.; Fukuzumi, S.; Crossley, M. J. *Chem. Commun.* **2002**, 356−357. (b) Ou, Z.; Kadish, K. M.; Wenbo, E.; Shao, J.; Sintic, P. J.; Ohkubo, K.; Fukuzumi, S.; Crossley, M. J. *Inorg. Chem.* **2004**, *43*, 2078.
(26) Kumar, A.; Neta, P. *J. Phys. Chem.* **1981**, *85*, 2830.
(27) Kadish, K. M.; Lin, X. Q.; Ding, J. Q.; Wu, Y. T.; Araullo, C. *Inorg. Chem.* **1986**, *25*, 3236.

Table 2. UV−Vis Spectral Data for the Neutral and Two-Electron Reduced Products of $[(TMpyP)M]^{n+}$ in DMF, 0.2 M TBAP

		electrode reduction λ, nm ($\epsilon \times 10^{-3}$ M^{-1} cm^{-1})					
		neutral			$2e^-$ reduced		
group	metal				band I	band II	ϵ_{II}/ϵ_I
A	Cu^{II}	424 (170)	545 (11.7)	580 (5.2)	477 (40.5)	814 (47.5)	1.17
	Ga^{III}	432 (164)	558 (10.6)	602 (3.0)	478 (45.4)	828 (53.0)	1.17
	In^{III}	434 (167)	564 (8.8)	604 (5.3)	486 (28.1)	805 (28.1)	1.00
	Ni^{II}	419 (134)	531 (10.3)	571 (3.2)	481 (32.5)	844 (34.6)	1.06
	Pb^{II}	478 (127)	550 (10.5)	564 (5.2)	478 (53.6)	771 (58.2)	1.09
	Pd^{IIa}	418 (178)	525 (15.9)	557 (6.3)	486 (67.5)	820 (63.4)	0.94
	Pt^{II}	403 (116)	513 (11.3)	544 (7.2)	487 (28.9)	829 (25.8)	0.89
	$V^{IV}O^a$	438 (230)	562 (14.6)	601 (2.9)	494 (95.8)	852 (106.5)	1.11
	Mg^{II}	443 (147)	575 (11.7)	622 (5.8)	469 (73.9)	742 (61.8)	0.84
B	Zn^{II}	446 (207)	568 (16.6)	620 (7.4)	469 (73.9)	772 (75.7)	1.02
	$Cd^{II\,a}$	453 (100)	583 (9.2)	630 (6.3)	466 (46.1)	764 (47.9)	1.04

[a] 0.1 M TBAP.

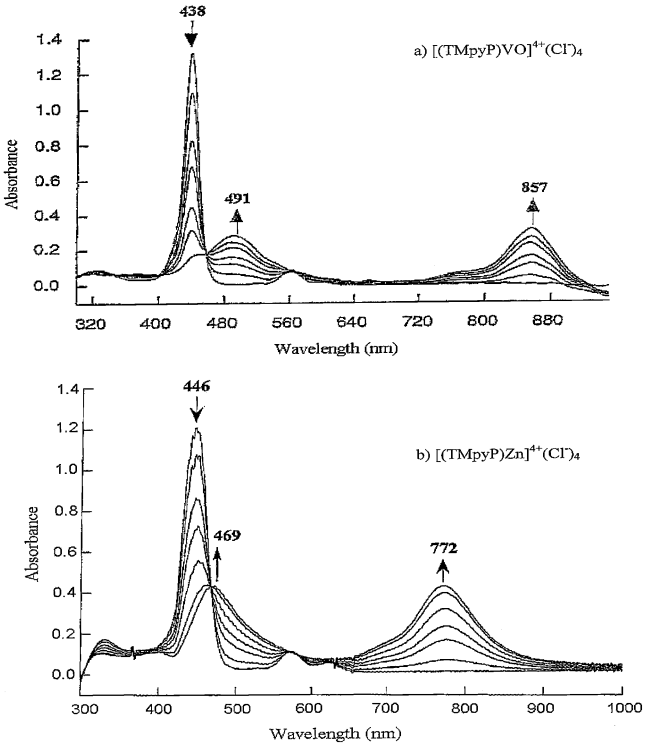

Figure 7. Time-resolved thin-layer UV−vis spectral changes upon the first reduction of (a) $[(TMpyP)VO]^{4+}(Cl^-)_4$ and (b) $[(TMpyP)Zn]^{4+}(Cl^-)_4$.

species are rather scarce in the literature, and those which have been spectrally characterized show absorption bands at 530−560 and 580−610 nm[28] with no features between 750 and 850 nm as is the case for the two-electron reduced forms of each group A and B porphyrin. In fact, those absorption bands are of similar magnitude and are rather reminiscent of phlorin dianions[29] and bacteriochlorins[30,31] where there is interruption of the π-system. This unusual feature of the TMpyP porphyrin dianions could thus be accounted for by the fact that electron delocalization between the positive charge and the π-ring system might be also interrupted once two electrons are added to the macrocycle.

It is noteworthy that the large molar absorptivity of the absorption band at 750−850 nm could also make the doubly reduced form of the TMpyP derivatives attractive candidates for photodynamic therapy since porphyrins usually lack absorption bands in the near-infrared.

The last two reductions of $[(TMpyP)M]^{4+}(CH_3C_6H_4SO_3^-)_4$, where M = Cu, Zn, or VO, have been assigned as electrode processes involving the four 1-methyl-4-pyridyl substituents,[19] and a similar assignment can be proposed for the last two reductions of the group A compounds on the basis of their UV−vis spectroelectrochemical data and electrochemistry. The spectral changes that occur upon the second and third reductions of $[(TMpyP)Pd]^{4+}(Cl^-)_4$ in DMF, 0.2 M TBAP, are illustrated in Figure 8 as representative examples while Table 3 summarizes the UV−vis spectral data for the four- and six-electron reduced forms of selected group A compounds. The data in Figure 8 parallel what has been observed during the second and third reductions of $[(TMpyP)Cu]^{4+}(CH_3C_6H_4SO_3^-)_4$.[19] Furthermore, the four-electron reduced species of group A compounds in Table 3 exhibit similar spectral features; an intense absorption band at 428−448, a shoulder band at 545−558, and a weaker band in the near-infrared at 818−852 nm. In all cases, the higher energy band at 428−448 nm increases in intensity whereas the other two bands vanish upon going from the four-electron to the six-electron reduced forms of each group A compound.

Similar spectral features were also seen upon the third two-electron addition of $[(TMpyP)M]^{4+}(CH_3C_6H_4SO_3^-)_4$ where M = Cu, Zn, or VO.[19] Overall, the data in Figure 8 and Table 3 therefore indicate that the last two two-electron reductions of each group A compound both occur at the 1-methyl-4-pyridyl substituents.

In the case of group B compounds, it was not possible to observe the spectral changes during each process III, IV, and V because these are partially overlapped in potential. The spectral data of the six-electron reduced forms of the Zn and Cd derivatives can be compared to the UV−vis spectral features of the products obtained after the third reduction of the group A compounds since the overall reductions of group A and B compounds all involve the addition of six electrons on the porphyrin moiety. The six-electron reduction products of the group A compounds in Table 3 are characterized by one major band at 428−448 nm. These spectral

(28) Peychal-Heiling, G.; Wilson, G. S. *Anal. Chem.* **1971**, *43*, 550.
(29) Lanese, J. G.; Wilson, G. S. *J. Electrochem. Soc.* **1972**, *19*, 1039.
(30) Scheer, H.; Inhoffen, H. H. In *The Porphyrins*; Dolphin, D., Ed.; Academic Press: New York, 1978; Vol 2, p 45.
(31) Hasegawa, J.; Ozeki, Y.; Ohkawa, K.; Hada, M.; Nakatsuji, H. *J. Phys. Chem. B* **1998**, *102*, 1320.

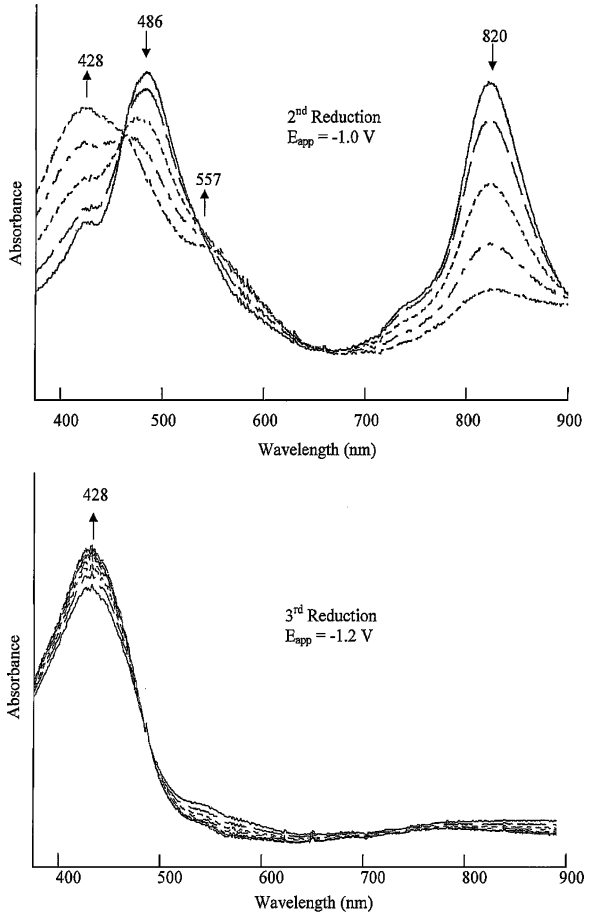

Figure 8. Time-resolved thin-layer UV−vis spectral changes upon the (a) second and (b) third reduction of $[(TMpyP)Pd]^{4+}(Cl^-)_4$ in DMF, 0.2 M TBAP.

Table 3. UV−Vis Spectral Data for the Four- and Six-Electron Reduced Products of Selected Group A Compounds in DMF, 0.1 or 0.2 M TBAP

		electrode reaction λ, nm ($\epsilon \times 10^{-3}$ M^{-1} cm^{-1})			
		4e⁻ reduced			6e⁻ reduced
group	metal				
A	Pd^{II}	428 (59.3)	557 (34.8)	820 (26.6)	428 (96.2)
	$V^{IV}O$	448 (87.3)	558 (76.7)	852 (68.1)	448 (102.2)
	Cu^{II}	428 (30.9)	545 (11.7)	818 (23.2)	428 (67.1)

features are also seen in the six-electron reduced forms of $[(TMpyP)Zn]^{4+}(BPh_4^-)_4$ and $[(TMpyP)Cd]^{4+}(BPh_4^-)_4$, thus confirming that, in the case of group B compounds, each process after the first reduction involves electron addition to the 1-methyl-4-pyridyl substituents.

The spectroelectrochemical properties of $[(TMpyP)MnCl]^{4+}(Cl^-)_4$ and $[(TMpyP)Co]^{4+}(Cl^-)_4$ have been previously discussed in the literature,[20,21] and the discussion of data in the present study will be limited to the Fe and Au derivatives.

Figure 9 illustrates the UV−vis spectral changes which occur during the first reduction of $[(TMpyP)FeCl]^{4+}(Cl^-)_4$ and $[(TMpyP)AuCl]^{4+}(Cl^-)_4$. The spectral data of the unreduced and the one-electron-reduced products of the group C compounds are summarized in Table 4. The Mn(III) and Co(II) derivatives each undergo an initial M(III)/M(II) electrode process,[20,21] and this is also clearly the case for

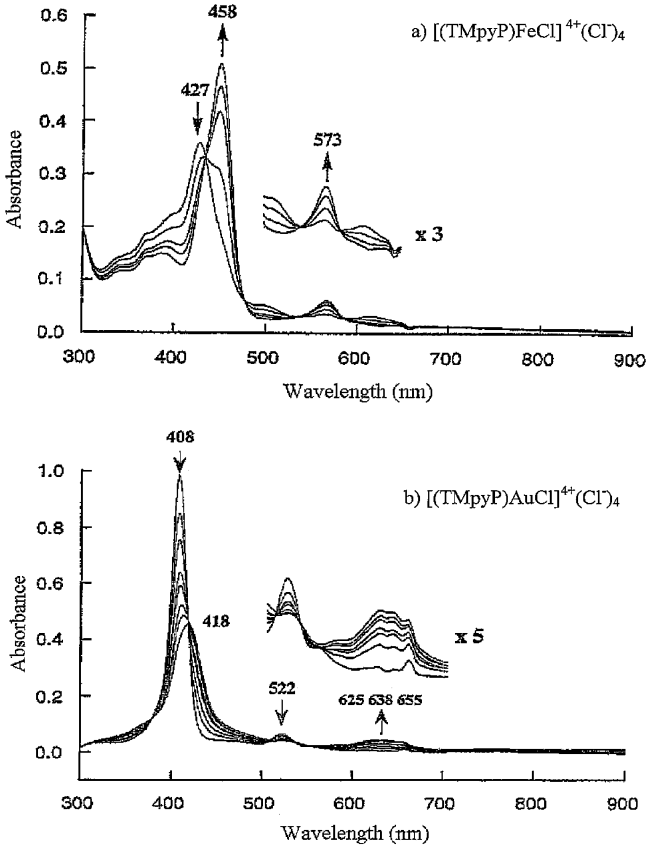

Figure 9. Time-resolved thin-layer UV−visi spectral changes upon the first reduction of (a) $[(TMpyP)FeCl]^{4+}(Cl^-)_4$ and (b) $[(TMpyP)AuCl]^{4+}(Cl^-)_4$ in DMF, 0.2 M TBAP.

Table 4. UV−Vis Spectral Data for the Neutral and One-Electron Reduced Forms of Group C Compounds

	electrode reaction λ, nm ($\epsilon \times 10^{-3}$ M^{-1} cm^{-1})					
	neutral			1e⁻ reduced		
metal						
Mn^{III}	461(123.8)	580(12.4)	630(7.1)	463(82.1)	581(8.8)	618(5.3)
Fe^{III}	427(84.2)	499(8.8)	620(5.3)	458(127)	573(12.4)	
Au^{III}	408(167)	522(10.5)		418(53.6)		640(9.4)[a]
Co^{III}	441(105)	558(11.7)		426(101)	537(9.0)	

[a] Broad band.

the Fe(III) derivative. As seen in Figure 9a, the Soret band of the iron derivative increases in intensity and shifts from 427 to 458 nm upon reduction while at the same time a weak visible band at 573 nm increases in intensity; similar trends are usually observed for the Fe(III)/Fe(II) couple of other iron porphyrins.[32]

The second reduction of $[(TMpyP)MnCl]^{4+}(Cl^-)_4$ is known to involve two electrons,[21] and a similar assignment can be proposed for the second reduction of $[(TMpyP)FeCl]^{4+}(Cl^-)_4$ on the basis of the cyclic voltammetric data discussed earlier in this manuscript. The UV−vis spectral changes obtained upon the second reduction of $[(TMpyP)FeCl]^{4+}(Cl^-)_4$ are shown in Figure 10. The Soret band decreased in intensity and shifted from 458 to 466 nm as the reduction proceeded. At the same time, a new band developed at 776 nm. These

(32) Kadish, K. M.; Van Caemelbecke, E.; D'Souza, F.; Lin, M.; Nurco, D. J.; Medforth, C. J.; Forsyth, T. P.; Krattinger, B.; Smith, K. M.; Fukuzumi, S.; Nakanishi, I.; Shelnutt, J. A. *Inorg. Chem.* **1999**, *38*, 2188.

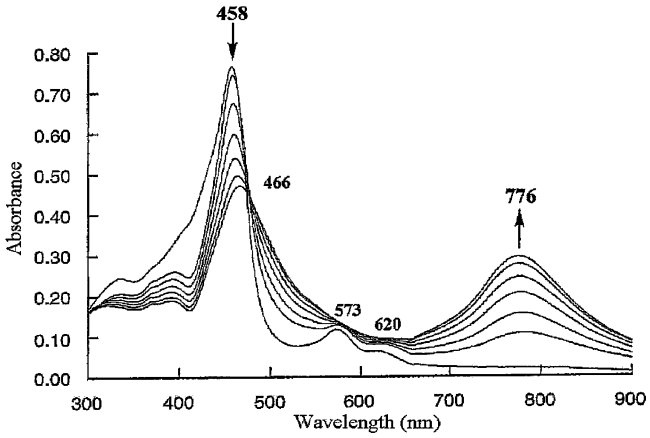

Figure 10. Time-resolved thin-layer UV−vis spectral changes upon the second reduction of $[(TMpyP)FeCl]^{4+}(Cl^-)_4$ in DMF, 0.2 M TBAP.

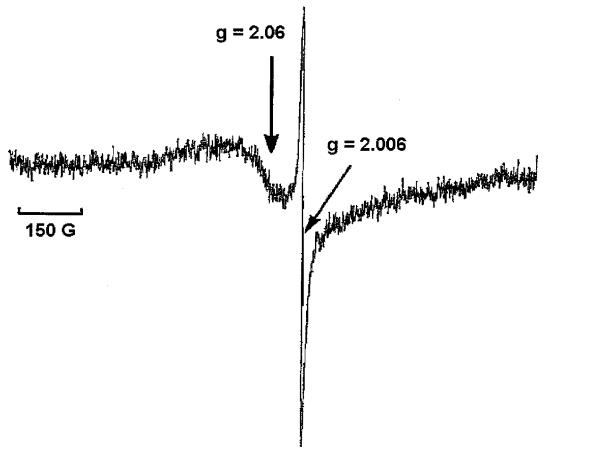

Figure 11. ESR spectrum of singly reduced $[(TMpyP)AuCl]^{4+}(Cl^-)_4$ (2.0×10^{-4} M) generated by the addition of 1 equiv of naphthalene radical anion (2.0×10^{-4} M) in DMF at −160 °C.

changes resemble what is observed upon conversion of $[(TMpyP)Zn]^{4+}(Cl^-)_4$ to its dianionic form (see Figure 7b), thus suggesting that the second reduction product of $[(TMpyP)FeCl]^{4+}(Cl^-)_4$, i.e., the species electrogenerated after process II in Figure 5b, is an iron(II) porphyrin dianion. As discussed earlier in the manuscript, the iron(II) dianion can be reduced by four more electrons, each of which is proposed to be added on the $N-CH_3^+$ group of the porphyrin. The spectral changes which occur upon the first reduction of $[(TMpyP)AuCl]^{4+}(Cl^-)_4$ are illustrated in Figure 9b. As seen in this figure, the Soret band decreases only slightly in intensity and shifts from 408 to 418 nm during the first one-electron addition, while at the same time, one broad band grows in at 625−655 nm. A similar spectral change has been reported for gold porphyrins with substituted TPP macrocycles.[25] The changes in the Soret region suggest a metal-centered electrode process, but the features in the visible region might also be accounted for by a macrocycle-centered process.[22] Therefore, on the basis of the spectroelectrochemical data and data on other Au(III) porphyrins, one can formulate the reduced form of $[(TMpyP)AuCl]^{4+}(Cl^-)_4$ as a gold(II) porphyrin with some π-anion radical character.

This assignment was also confirmed by the ESR spectrum of $[(TMpyP)Au]^{4+}$, a compound which was chemically generated by addition of 1 equiv of naphthalene radical anion to a frozen DMF solution of $[(TMpyP)AuCl]^{4+}(Cl^-)_4$. The ESR spectrum of $[(TMpyP)Au]^{4+}$ is shown in Figure 11 and exhibits a broad signal centered at $g = 2.06$ on which is superimposed a sharp signal centered at $g = 2.006$. The first feature of the spectrum is consistent with the presence of gold(II) in the reduced form of the compound[25] while the other feature suggests a gold(III) π-anion radical.[22,33] The amount of gold(II) was estimated as 97% based on the double integration of the two signals, thus indicating that in the reduced form of the porphyrin gold(II) dominates over gold(III) π-anion radical in a ratio of about 97:3.

Summary

Sixteen different complexes of the type $[(TMpyP)M]^{4+}(X^-)_4$ or $[(TMpyP)MCl]^{4+}(Cl^-)_4$ ($X^- = Cl^-$ or BPh_4^-, M = M(II) or M(III)) were investigated as to their electrochemical properties in *N*,*N*-dimethylformamide in order to examine how the electrochemical behavior of a series of TMpyP porphyrins changes with the metal ion and/or the counterion. All investigated compounds with M(II) or electroinactive M(III) central metals can be reduced by an overall six electrons. The first two-electron reduction yields a porphyrin dianion with unusual spectral properties, and this is followed by further reductions of the 1-methyl-4-pyridyl substituents at more negative potentials. However, the exact number of redox processes and their reversibility appear to be functions of the metal ion electronegativity[34] and/or the type of counterion. More specifically, all (TMpyP)M porphyrins containing a metal ion whose electronegativity ranges from 1.52 to 1.74 undergoes three reversible two-electron-transfer processes but up to four processes involving an overall transfer of six electrons can be seen for compounds whose central metal ions electronegativity fall in the range 1.17−1.34. When the central metal ion is an electroactive M(III) ion, the porphyrin undergoes an M(III)/M(II) process prior to electrode reactions involving the porphyrin π-ring system and/or the 1-methyl-4-pyridyl substituents, but the exact type of electron transfer mechanism will depend on the metal ion.

The type of counterion has virtually no effect on the electrochemistry of (TMpyP)M complexes when the metal ion electronegativity ranges from 1.52 to 1.74, with the only exception being the Ni derivative. A different trend is seen for porphyrins whose central metal ions have a lower electronegativity, such as $[(TMpyP)Zn]^{4+}(X^-)_4$ ($X^- = Cl^-$ or BPh_4^-). In this case, the electron transfer processes involving the 1-methyl-4-pyridyl groups depend on the porphyrin counterion.

Acknowledgment. The support of the Robert A. Welch Foundation (K.M.K., Grant E-680) is gratefully acknowledged.

IC048820Q

(33) The *g* value of the sharp signal (2.006) is clearly different from that of the naphthalene radical anion (2.002).

(34) Portier, J.; Campet, G.; Etourneau, J.; Tanguy, B. *J. Alloys Compd.* **1994**, *209*, 285.